

A COMPUTATIONAL FRAMEWORK FOR MODELING EMERGENCE OF COLOR VISION IN THE HUMAN BRAIN

Anonymous authors

Paper under double-blind review

ABSTRACT

It is a mystery how the brain decodes color vision purely from the optic nerve signals it receives, with a core inferential challenge being how it disentangles internal perception with the correct color dimensionality from the unknown encoding properties of the eye. In this paper, we introduce a computational framework for modeling this emergence of human color vision by simulating both the eye and the cortex. Existing research often overlooks how the cortex develops color vision or represents color space internally, assuming that the color dimensionality is known a priori; however, we argue that the visual cortex has the capability and the challenge of inferring the color dimensionality purely from fluctuations in the optic nerve signals. To validate our theory, we introduce a simulation engine for biological eyes based on established vision science and generate optic nerve signals resulting from looking at natural images. Further, we propose a bio-plausible model of cortical learning based on self-supervised prediction of optic nerve signal fluctuations under natural eye motions. We show that this model naturally learns to generate color vision by disentangling retinal invariants from the sensory signals. When the retina contains N types of color photoreceptors, our simulation shows that N -dimensional color vision naturally emerges, verified through formal colorimetry. Using this framework, we also present the first simulation work that successfully boosts the color dimensionality, as observed in gene therapy on squirrel monkeys, and demonstrates the possibility of enhancing human color vision from 3D to 4D.

1 INTRODUCTION

“Color is the place where our brain and the universe meet.” – Paul Klee

We experience colors in everyday life so effortlessly that it is easy to take the underlying neural computations for granted. In fact, the sensory signals exiting our eye, called optic nerve signals (ONS), are nothing like our color vision (see Fig. 1 and Video 0:13). For example, ONS are spatially warped, akin to an image taken with a fish-eye lens, due to varying densities of photoreceptor cells in the retina (Curcio et al., 1990). ONS does not come in color either – colors of the scene are spectrally sampled by different types of color sensitive cells (cone cells) in the retina, appearing as a layer of spatial noise in the ONS. Furthermore, other processes, such as lateral inhibition and action potentials, render the image structure barely recognizable, in gradient domain where spatiotemporal “edges” dominate. Now, the question is: *how are we still seeing colors?*

Specifically, this paper introduces a novel computational framework for modeling the emergence of human color vision by simulating the eye and the cortex. For the eye, we present a biophysically accurate implementation of a textbook scientific model of the retinal neural circuitry. For the brain, we hypothesize a low-level, self-supervised learning mechanism in the cortex that operates purely on the optic nerve signal stream. For color representation in the brain, we propose modeling color in the brain as a high-dimensional vector, rather than assuming any specific color dimensionality and show that the correct color dimensionality emerges naturally through the proposed learning.

For eye simulation, our goal is to create a computational engine that takes in any spectral image of the world and outputs the corresponding optic nerve signal stream, based on established vision science. Our model captures how scene form, color, and motion become spatiotemporally entangled in the optic nerve signal stream. Our simulation is based on the “textbook” model of vision science (Rodieck 1998) for midget, private-line visual pathways, detailed in Section 3, and comprising fixational eye motion, spectral encoding by cone cells, foveation, and lateral inhibition.

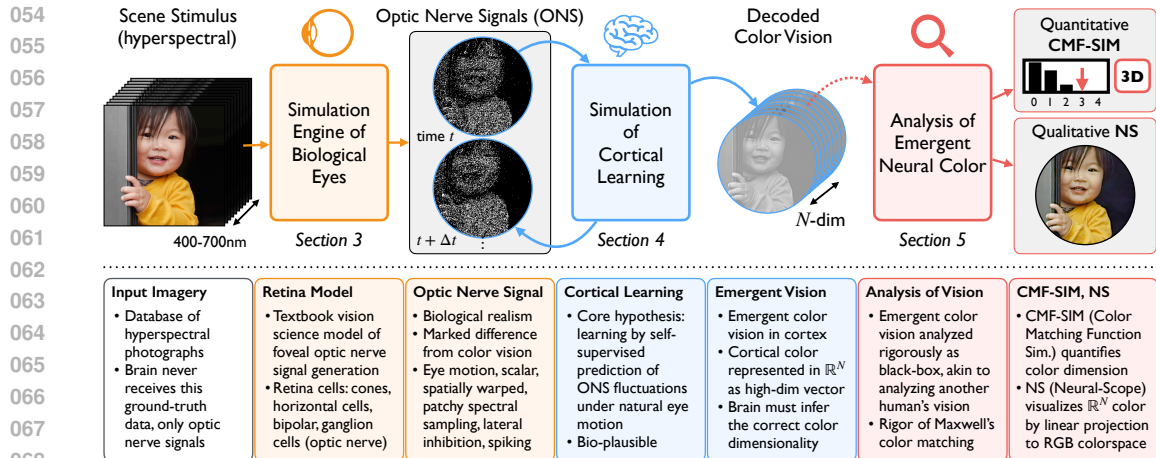


Figure 1: Overview of our proposed framework for modeling the emergence of human color vision. Our simulation engine of biological eyes converts a scene stimulus (hyperspectral image) to a stream of optic nerve signals (Section 3 & Video 0:13). We simulate cortical learning purely from these optic nerve signals (Section 4) and show the emergence of color vision. We show how to analyze the emergent neural color quantitatively with Color Matching Function test Simulator (*CMF-SIM*) and qualitatively with Neural Scope (*NS*) (Section 5).

For brain simulation, we hypothesize that the cortex could disentangle the optic nerve signal from the invariant retinal properties to generate color vision – purely through a self-supervised learning process that aims to predict the constant fluctuations in cellular-level activations of the optic nerve signal during small eye movements. The neural conditions for such self-supervised learning are biologically plausible in the sense that the cortex continuously receives optic nerve signals under the tiny gaze movements of fixational eye drift. The theoretical intuition for why such learning might succeed is that eye motion repeatedly draws a static scene image across the invariant spectral and spatial sampling properties of the retina, potentially enabling the retinal properties and scene images to be mutually filtered out of the optic nerve signal where they are entangled. We show that this simple learning mechanism succeeds at discovering color vision with the correct dimensionality.

But first, a somewhat esoteric yet technically critical feature of the modeling framework needs discussion: color representation in the brain. Existing research often overlooks how the cortex develops color vision or represents color space internally, assuming that the color dimensionality is known a priori, e.g. RGB. We argue that the cortex has the capability and the task of inferring color dimensionality, purely from fluctuations in the optic nerve signals. Therefore, we propose representing color in the cortex as a high-dimensional vector in \mathbb{R}^N and find that the correct color space and color dimensionality emerge naturally as geometric properties of the hypothesized learning mechanism. We show how to formally quantify and visualize the emergent color space (Section 5).

Remarkably, the hypothesized learning mechanism results in clear color vision of the correct color dimensionality. When the retina contains 1, 2, 3 or 4 types of color photoreceptors (cones), correct color dimensionality emerges: respectively, 1D mono-, 2D di-, 3D tri- or 4D tetra-chromatic vision. In fact, it is an esoteric but well-known fact in vision science that the three types of 2D dichromacy result in highly specific color-spaces (blue-yellow, blue-orange, and teal-pink), which we see emerge naturally. Even more, the simulation presents a model of how color dimensionality boosting occurred in the squirrel monkeys (Mancuso et al., 2009). We simulate injection of the third cone pigment virus into the dichromat retina, which results in boosting from dichromacy to trichromacy. Intriguingly, the model also shows the possibility that normal human trichromacy could be boosted to tetrachromacy.

In sum, our proposed framework formulates the emergence of human color vision in a computational manner. The simulation engine of realistic optic nerve signals generates training data to this problem, and an intentional and challenging constraint is that the cortical model must strictly learn only from the optic nerve signal with no auxiliary information. This paper presents the first, simple and yet complete existence proof that such cortical inference is possible, and we show that this learning simulation is consistent with various surprising and unexplained vision science phenomena.

2 RELATED WORK

2.1 VISION SCIENCE ON OPTIC NERVE SIGNAL ENCODING

In the “textbook” model, the retina transforms light into electrical signals through three primary functions: color sampling via cone cell spectral response functions, lateral inhibition via horizontal neural connections, and spatial sampling via cell positioning (Fig. 2). Under daylight, this process begins when light activates cone cells, which are of three types for most humans (Young, 1801, 1802; Von Helmholtz, 1867), each sensitive to different wavelengths (Stockman & Sharpe, 2000). These signals are then modulated by horizontal cells that enhance visual contrast through lateral inhibition (Rodieck, 1965; Dacey et al., 1996; Verweij et al., 2003). The signals continue to bipolar and retinal ganglion cells (RGCs), with a direct connection in the fovea via the midget private-line pathway (Dowling & Boycott, 1966; McMahon et al., 2000; Wool et al., 2018), vital for high-resolution color vision. Notably, the cone cell density varies, reaching its peak in the fovea (Osterberg, 1935; Curcio et al., 1990). The axons of the ganglion cells bundle to form optic nerve signals, maintaining their spatial arrangement, which results in a retinotopy in the visual cortex (Holmes, 1918; Tootell et al., 1982; Dougherty et al., 2003). Fixational eye movements cause dynamic photoreceptor activation at all times by constantly shifting the gaze, even when focusing on static objects (Rucci & Victor, 2015; Young & Smithson, 2021; Martinez-Conde et al., 2013).

Recordings of real optic nerve signals exist, but cannot be used for our cortical simulations because they are orders of magnitude too low resolution (from only a few thousand cells) and only in response to grayscale rather than color imagery (Litke et al., 2004; Brackbill et al., 2020; Marre et al., 2017; Liu et al., 2022). To overcome these data limitations, we present a simulation engine for the midget private-line pathway in the fovea in Section 3.

2.2 COLOR REPRESENTATION IN COMPUTATIONAL NEUROSCIENCE

It is an open question how to meaningfully model neural representations of color in simulations of visual perception. Most computational neuroscience sidesteps this issue, “hard-coding” a dimensionality of 3, representing and constraining cortical color to tristimulus values, such as RGB (Parthasarathy et al., 2017; Botella-Soler et al., 2018; Brackbill et al., 2020; Kim et al., 2021; Zhang et al., 2022; Wu et al., 2022), LMS (Young, 1802; Von Helmholtz, 1867) or cone-opponent space (Derrington et al., 1984; MacLeod & Boynton, 1979). Constraining cortical models to such a ceiling of three for dimensionality clearly conflicts with the study of a functional tetrachromat observer with 4D color vision (Jordan et al., 2010; Rezeanu et al., 2021). Instead, we model the brain with the capability and the challenge of deducing the inherent color dimensionality encoded in the optic nerve signals.

2.3 THEORY ON HOW VISION EMERGES IN THE BRAIN

In computational vision science modeling, it is often overlooked that the cortex relies solely on a stream of optic nerve signals to discover color vision, with no access to a teacher signal or perceptual ground truth. Rather, various efforts have been made to reconstruct visual stimuli from neural responses by giving the cortical model access to ground truth stimulus image (Naselaris et al., 2009; Nishimoto et al., 2011; Parthasarathy et al., 2017; Botella-Soler et al., 2018; Brackbill et al., 2020; Kim et al., 2021), but the neural reality is that the brain never has direct access to the visual scene. This characteristic makes the human visual system a quintessential example of self-supervised learning, which is a growing field in computer vision (De Sa, 1993; Chen et al., 2020; He et al., 2022). In this work, we propose a learning principle in the cortex which aims to predict the cellular-level fluctuations in activation that occur during small eye movements, which is associated with the idea of temporal prediction (Palmer et al., 2015; Lotter et al., 2016; Singer et al., 2018, 2023b), as well as the broader concept of predictive coding (Rao & Ballard, 1999; Srinivasan et al., 1982). It is also closely linked to the sensorimotor contingency theory from cognitive science (O’Regan & Noë, 2001) and slow feature analysis (Hinton, 1990; Földiák, 1991) which suggests that the brain learns to anticipate the sensory outcomes of motor actions (e.g. eye movements) and utilizes these anticipations to filter out invariant (slow) features.

2.4 THEORY ON HOW BRAINS INFER COLOR DIMENSIONALITY

Previous studies has investigated inference of invariant retinal properties from sensory signals. For instance, research has demonstrated the ability to deduce cone cell types (Wachtler et al., 2007; Brainard et al., 2008; Benson et al., 2014) and the positions of photoreceptors (Maloney & Ahumada, 1989; Brainard et al., 2008) via statistical methods from sensory signals. Brainard et al. (2008) hinted at analyzing sensory inputs from different time points during fixational drift as a way to reveal retinal features, and in this paper we provide a computational realization of this idea with a specific learning mechanism that achieves complete disentanglement of retinal invariants from optic nerve signals.

2.5 MEASUREMENT OF COLOR DIMENSIONALITY IN HUMAN COLOR PERCEPTION

In this paper, we need to rigorously measure the color dimensionality of the emergent color from cortical simulation. To do so, we adapt Maxwell’s famous color-matching experiments (Maxwell, 1856), which laid the foundation of colorimetry that remains at the heart of all color reproduction technology today. Color matching experiments confirmed the trichromatic theory (Young, 1802; Von Helmholtz, 1867; Grassmann, 1853) in which the 3-dimensional nature of human color vision has its basis in the three different cone types in the human retina. Jacobs’s recent review (Jacobs, 2018) of color dimensionality in animal vision, however, reminds the community that the dimensionality of color vision does not automatically equal the number of cone types, and that the most rigorous way to measure it remains Maxwellian color matching – as we follow in this work.

2.6 COMPLEXITY OF HUMAN COLOR VISION

This paper focuses on color dimensionality because it is the foundational characteristic of an observer’s color experience, but many layers of further perceptual complexity exist atop that foundation. Examples include chromatic adaptation (color constancy) (Von Kries, 1902; Land, 1977; Foster, 2011), perceptual nonuniformity across colorspace (CIE, 1976; MacAdam, 1942), complex contextual interactions (Fairchild, 2013), and even surprising flood-fill features (Pinna, 1987; Pinna et al., 2001). Parts of these perceptual phenomena are scientifically mapped to neural correlates, such as nonlinear photoreceptor responses (Krauskopf & Karl, 1992; Angueyra et al., 2022), or parvocellular pathway and neural processes spanning V1, V2, and V4 (Livingstone & Hubel, 1987; Zeki, 1978; Li et al., 2014; Liu et al., 2020; Angueyra et al., 2022). This paper leaves these additional layers of perceptual complexity as future modeling work.

3 SIMULATION ENGINE FOR BIOLOGICAL EYES AND OPTIC NERVE SIGNALS

We model the primary functions of the human retina based on the known science. The inputs to our retina model are hyperspectral images (Fig. 2.A; details in Appendix A.1). A model of fixational eye drift (Rucci & Victor, 2015; Young & Smithson, 2021; Martinez-Conde et al., 2013) generates a sequence of frames that sample different parts of the image. Each frame is projected on the retina, stimulating a randomized array of cone cells, according to known cell density variation as a function of eccentricity (distance from the fovea) (Curcio et al., 1990) and known statistics of different cone cell types (Carroll et al., 2000) (Fig. 2.B). Each cone cell converts the scene light into photoreceptor activations based on cone type spectral response functions (Stockman et al., 1999; Stockman & Sharpe, 2000) (Fig. 2.C), followed by lateral inhibition from horizontal cells (Wool et al., 2018; Rodieck, 1965) (Fig. 2.D). These signals are transformed into spike trains (Fig. 2.E), then bundled into optic nerve signals (ONS), resulting in spatial distortion (Fig. 2.F), turning a color scene stimulus into a noisy, spatially distorted ONS. Additional details are in Appendix A and Video 1:15.

One observation to make is that there are three invariant properties of the simulated retina (i.e. retinal invariants): cell positions, cell types, and horizontal cell connections. These properties are held constant during generation of ONS for a particular eye, but we use the engine with different values for these properties to generate ONS datasets for a diverse set of eyes. For example, we create datasets with different cone types, including monochromatic (L, M, S), dichromatic (LM, LS, MS), trichromatic (LMS) and tetrachromatic (LMSQ) configurations (Fig. 2.4). The generated ONS becomes spatially noisier as the number of cone types increases, and we investigate how the cortex infers the inherent color dimensionality of these eyes purely from the encoded differences in their respective ONS. We will release the dataset and code for generating ONS upon acceptance.

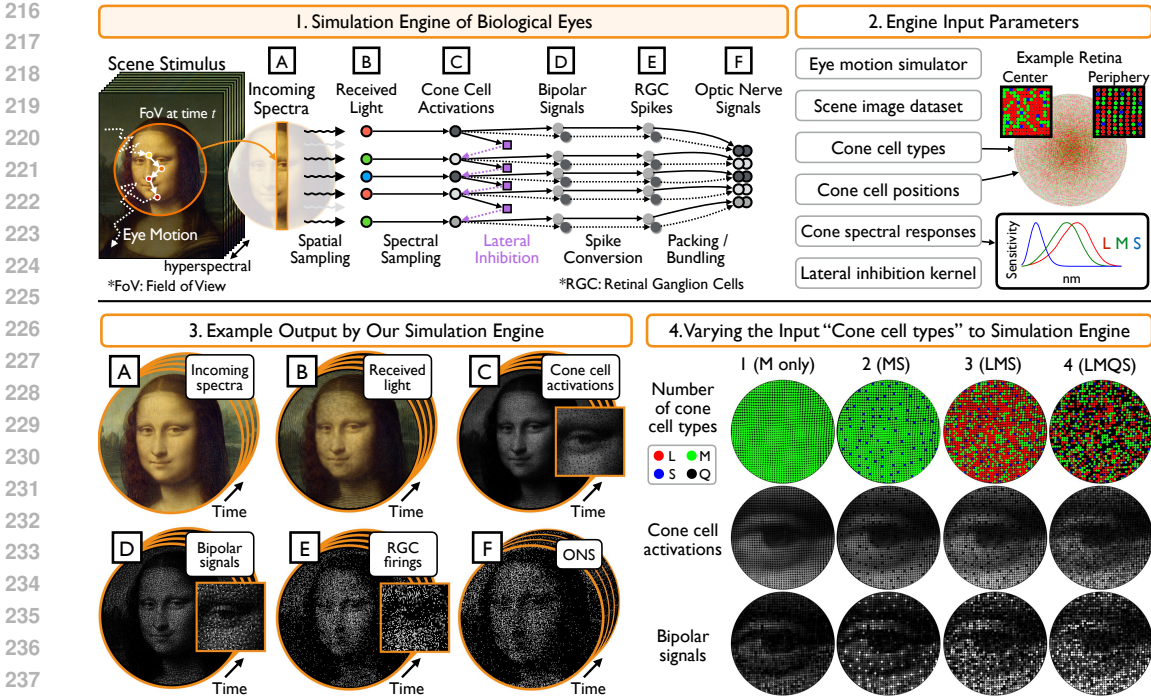


Figure 2: Overview of our simulation engine of biological eyes. 1. This engine takes a scene stimulus as an input, processes it through a “textbook” model of eye motion and retinal neural circuitry, to generate a stream of optic nerve signals. 2. This engine accepts custom eye and retina parameters. 3. It allows visualization of neural signals in steps (A-F), illustrating the progressive entanglement of scene imagery with retinal properties. 4. Visualization of changing one of the input parameters, the number of cone cell types – showing that the signals become noisier as the number increases.

4 SIMULATING CORTICAL LEARNING AND EMERGENCE OF COLOR VISION

Our cortical model is structured to learn three functions in a pipeline (Fig. 3.1): 1. Φ that decodes the optic nerve signal at time t into its internal percept; 2. Ω that translates this percept according to eye motions inferred from the signal over a short time interval, dt ; and 3. Ψ that re-encodes the translated percept back into a predicted optic nerve signal at time $t + dt$, which is compared against the real signal received at that time. Mathematically, given the optic nerve signal O_t at time t ;

$$\hat{O}_{t+dt} = \Psi(\Omega(\Phi(O_t))) \quad (1)$$

where \hat{O}_{t+dt} is the predicted ONS at time $t + dt$. Here the task of decoder Φ is analogous to inverting the retinal processes to transform O_t into the visual percept image V_t (i.e. $V_t \leftarrow \Phi(O_t)$). Likewise, the re-encoder function Ψ resembles the retinal processes, as it aims to reproduce an optic nerve signal from the visual percept (i.e. $O_t \leftarrow \Psi(V_t)$). Therefore, Φ and Ψ are pseudo-inverses.

The learning objective is to minimize the prediction error $E_{\text{prediction}}$, the difference between predicted and real optic nerve images at time $t + dt$, such that:

$$E_{\text{prediction}} = \|O_{t+dt} - \hat{O}_{t+dt}\|_2^2 = \|O_{t+dt} - \Psi(\Omega(\Phi(O_t)))\|_2^2 \quad (2)$$

where O_{t+dt} is the real observed ONS at time $t + dt$.

Three main ideas drove the evolution of our selected model features. First, we reasoned that it would be a big step towards successful decoding and re-encoding if the cortex could infer the key encoding properties of each cone cell. We gave the cortical model sets of learnable parameters, which we call “neural buckets”, in which to store and update guesses of these properties during learning. The buckets contain the following information for each cone cell: 2D position in visual space (P), cone spectral identity (C), and lateral inhibition weights (W) to neighboring cones.

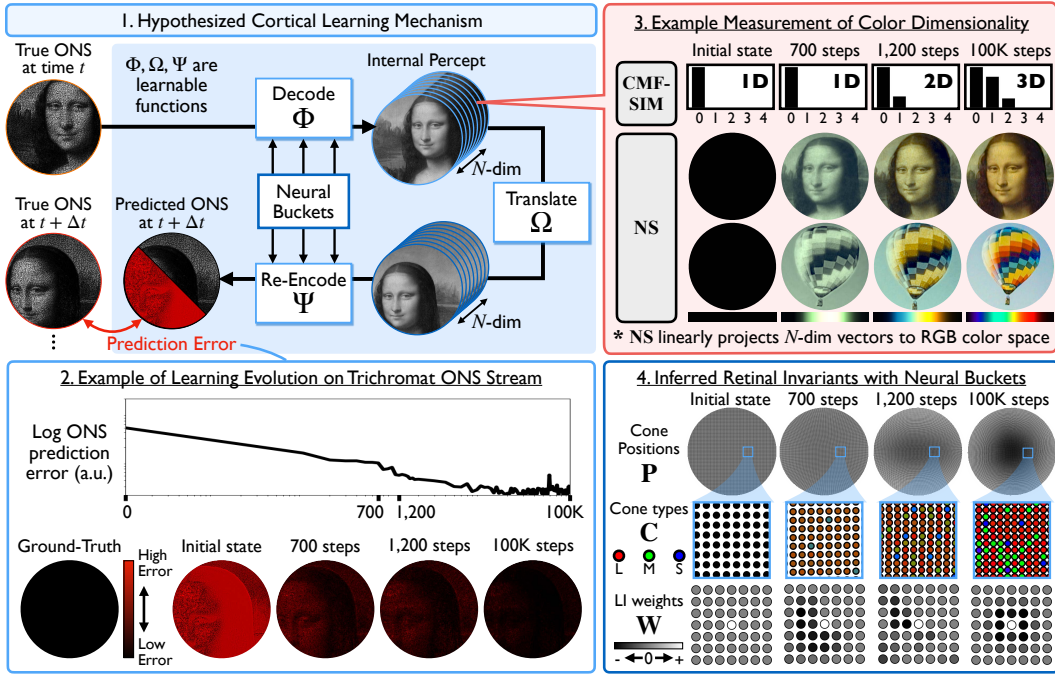


Figure 3: Overview of our hypothesized cortical learning mechanism and exclusive study of the learning behavior of the cortical model with trichromatic retina. 1. Given the stream of optic nerve signals as the only input data, the cortical model aims to predict the next ONS from the current one with 3 learnable functions, decoder Φ , translation operator Ω and re-encoder Ψ . 2. Prediction error decreases as learning progresses, converging after 100K learning steps. 3. During learning, the color dimensionality of the internal percepts transition from 1D, 2D to 3D, formally measured by *CMF-SIM* and visualized by *NS* (Fig. 4 & Section 5). 4. The cortical model infers the retinal invariant properties during learning: cell positions P (higher density in fovea), cone cell types C , and lateral inhibition weights W (center-surround receptive field).

The second main idea was the observation that decoder Φ and encoder Ψ are mathematically factorizable into a pipeline of subfunctions, such that:

$$\begin{aligned}\Phi &= \Phi_P \circ \Phi_C \circ \Phi_W \\ \Psi &= \Psi_W \circ \Psi_C \circ \Psi_P.\end{aligned}$$

Each sub-function is an operator conditioned on its corresponding neural bucket, cell positions P , cone spectral types C , and lateral inhibition weights to neighboring cells W . In case of decoder Φ , it first executes inversion of lateral inhibition using Φ_W in order to estimate the activations of each photoreceptor associated with an optic nerve axon; second, projects scalar cone activations into \mathbb{R}^N by Φ_C using inferred spectral identities in C (and interpolating color across space – the third main idea below); and finally inverting the spatial distortion of foveation via Φ_P . The re-encoding function is a pipeline of analogous subfunctions in reverse order: re-applying spatial warping with Ψ_P ; re-projecting color into scalar photoreceptor activations with Ψ_C ; and re-applying lateral inhibition with Ψ_W . Further implementation details are provided in Appendix B.

The third main idea was that, in order to accurately re-encode after translation, the model needs to learn to interpolate color information spatially, because there is only one cone type at each point on the retina. This need to interpolate is analogous to the situation in cameras with image sensors (Bayer, 1976; Fossum, 1997; Kimmel, 1999) that physically sample only one of the R,G,B channels at each pixel, and fundamentally require demosaicking algorithms to interpolate full R,G,B values at all pixels. The required interpolation function in the cortical model is more complex because the spectral sampling pattern is random, so learning this function is entangled with correctly resolving C . We enable and force the cortical model to learn the color interpolation function by representing it as a convolutional neural network with neural bucket parameters D (Appendix B.2.2).

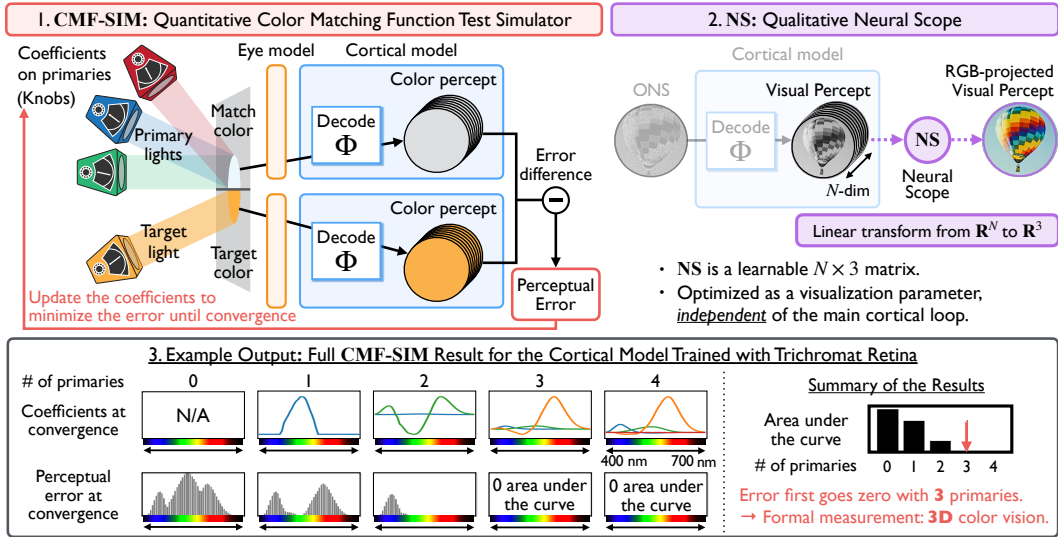


Figure 4: Overview of our measurement methods of emergent color dimensionality, Color Matching Function Test Simulator (*CMF-SIM*) & Neural Scope (*NS*). 1. *CMF-SIM* determines the minimum number of primary colors needed to match any target color by iteratively updating coefficients to minimize perceptual error. 2. *NS* visualizes visual percepts independently of the cortical learning loop, optimized as a learnable $N \times 3$ matrix to minimize projection error to the target RGB image. 3. Example *CMF-SIM* output for a trichromat retina-trained cortical model shows matching errors for 400–700nm spectral light converging to zero with three primaries, confirming 3D color vision.

An important detail is the handling of eye motion in the simulation. In one experiment we show that the model can learn a subfunction that estimates the eye motion translation between times t and $t + dt$ purely from the optic nerve signals at those times. The main computational challenge here is the spatial warp in optic nerve signals. The uniform translation in stimulus space corresponds to a non-uniform translation in the optic nerve signal space, which makes the prediction of the eye motion dependent on the inference of cell positions P . We find that the cortical model iteratively updates the neural bucket P from imperfect initial eye motion estimate, which helps to improve the prediction of eye motion, and vice versa. This inference converges to the correct eye motion estimate, as the model learns to minimize prediction error (Appendix B.3).

With this pipeline of subfunctions and associated neural buckets, the hypothesized learning is equivalent to parallel numerical optimization of all neural buckets in striving to minimize prediction error. We simulate learning using stochastic gradient descent (Kingma & Ba, 2014).

5 NEURAL REPRESENTATION OF COLOR SPACE AND ANALYSIS OF EMERGENT COLOR DIMENSIONALITY

We model color in the cortex as a vector in high-dimensional space, \mathbb{R}^N . This decision represents our view that the brain has both the freedom and the challenge of somehow inferring the intrinsic color dimensionality of the visual signals it is receiving along the optic nerve. Specifically, we define a cortical decoding function Φ that takes the optic nerve signal O_t at time t and transforms it into its internal visual percept V_t (Fig. 3), such that:

$$V_t = \Phi(O_t) \tag{3}$$

where each pixel in V_t is a N -dimensional vector. Inside \mathbb{R}^N , we assume that cortical color space emerges as a K -dimensional manifold. To measure this intrinsic dimensionality K , we introduce two methods: formal, numerical *CMF-SIM*; and intuitive, visual *NS*.

CMF-SIM (Color Matching Function Test Simulator) is our tool to formally quantify the color dimensionality that has emerged in the \mathbb{R}^N color space of the cortical model (Fig. 4.1). *CMF-SIM* treats the retina model and cortical model as a black-box color observer. Specifically, we limit

378 ourselves to showing the model two patches of scene color at random, distinct locations on the
 379 retina to reflect the effect of real-world viewing conditions, obtaining only a scalar score as feedback
 380 to indicate the difference in color appearance between the two patches (with zero representing a
 381 color match). This interface is intentionally limited and identical to color matching experiments
 382 with human subjects. Then, resting on the formal, technical bedrock for colorimetry established by
 383 Maxwell (1856) and Grassmann (1853), we exhaustively probe to determine the minimum number of
 384 color primaries needed to match any test color through linear combination (Fig. 4.1 & Appendix C).
 385 For example, Maxwell found that most humans require 3 primaries and are formally trichromatic, but
 386 red-green colorblind persons require only 2 primaries and are dichromatic. We model diverse color
 387 observers and measure the color dimensionality of their emergent vision.

388 NS (Neural-Scope) is our tool to display emergent colors in \mathbb{R}^N by projecting them into RGB color
 389 space (Fig. 4.2). NS is a learnable $N \times 3$ matrix mapping the emergent cortical color manifold in
 390 \mathbb{R}^N linearly to conventional RGB color, enabling visual inspection of emergent color vision. To
 391 compute NS , we first project our hyperspectral image dataset in two ways: (1) using the retina and
 392 learned cortical model to map hyperspectral images into the \mathbb{R}^N cortical colorspace, and (2) using
 393 conventional color processing to convert hyperspectral data to RGB via CIEXYZ (CIE, 1931). NS
 394 is then determined as the least squares transform from the former data in \mathbb{R}^N to the latter in RGB.
 395 Importantly, NS is independently optimized as a visualization parameter, separate from the main
 396 cortical loop, ensuring that the cortex processes ONS without any exposure to input images in either
 397 hyperspectral or RGB form. NS provides striking color visualizations and complementary intuition
 398 visually, which are fully consistent with formal $CMF-SIM$ results. For example, NS allows us to
 399 compute and contrast the color palettes of the three different types of human dichromacy (Fig. 5).

400 In sum, we model cortical color as vectors in \mathbb{R}^N , allow color space to emerge naturally through
 401 the hypothesized learning mechanism, and measure the emergent color space’s dimensionality
 402 quantitatively with $CMF-SIM$ and analyze it visually with NS .

404 6 SIMULATION RESULTS - EMERGENCE OF COLOR VISION

406 Figure 3.2 begins with a model of typical human retina containing L, M and S cones, and illustrates
 407 the time-varying behavior of the cortical model as it learns color vision. The visualized prediction
 408 error decreases as the training progresses, and the internal percept converges to 3-D color vision
 409 both formally ($CMF-SIM$) and visually (NS imagery), shown in Figure 3.3. Notably, the visual
 410 timeline highlights that the cortical model learns color vision one dimension at a time: achieving
 411 monochromacy at 700 learning steps, dichromacy at 1,200 steps, and converging to trichromacy after
 412 10^6 steps. At convergence, the cortical model has accurately inferred all retinal properties: spectral
 413 identity of each cell, cell positions and lateral inhibition neighbor weights (Fig. 3.4). For a cortical
 414 model trained with a trichromat retina, $CMF-SIM$ results closely align with human psychophysical
 415 data (Stiles & Burch, 1955) (Appendix G.1) and the model consistently demonstrates 3D color vision
 416 across different noise initializations (Appendix G.2), highlighting our model’s validity and robustness.

417 The remainder of this section shows $CMF-SIM$ and NS results at convergence for a diversity of
 418 simulation scenarios. Fig. 4.2 dissects the $CMF-SIM$ analysis for the case where the retina contains
 419 3 cone types. The graphs show color matching function results using optimal sets of color primaries
 420 from 0 to 4 primaries, along with the residual perceptual error as a function of wavelength. The area
 421 under the curve (AUC) for each error graph suggests that the error falls to near-zero only with at least
 422 3 primaries – this formally proves that the color dimensionality is 3.

423 Figure 5 presents results of the hypothesized cortical learning in a diversity of color observers
 424 where the retina contains different numbers of cone cell types. This shows that the model learns
 425 K -dimensional color vision when the retina contains K cone types. That is, when the retina contains
 426 1, 2, 3 or 4 cell types, the cortical model converges on mono, di, tri, or tetrachromat color vision,
 427 formally quantified with $CMF-SIM$ (further analysis of tetrachromat models in Appendix F). And
 428 qualitatively, we observe that the NS images are grayscale for $K = 1$, colorblind with only shades
 429 of blue and yellow for $K = 2$, and full color with all trichromatic hues only with $K = 3$ (Fig. 5.1).
 430 Use of NS is limited to color dimensionality up to 3, and is to not applicable to $K = 4$ case, but
 431 $CMF-SIM$ formally confirms that 4-dimensional color emerges there. All variants of retinas with
 two cone types (protanopia, deuteranopia and tritanopia), converge to 2D color vision. But more
 striking, NS reveals hue shifts among these models that are consistent with color vision deficiencies

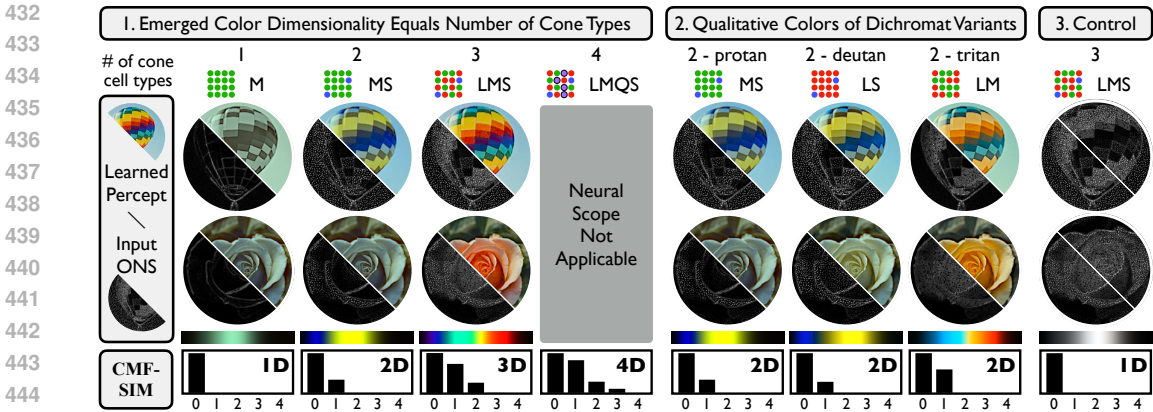


Figure 5: Results of simulating emergence of color vision from various retinas, with analysis of learned color dimensionality using qualitative visualization (*NS*) and formal methods (*CMF-SIM*). 1. Cortical models trained with dataset generated with retinas containing 1, 2, 3, 4 cone types result in mono-, di-, tri-, tetrachromatic color vision, respectively. 2. Qualitative color of dichromat variants is consistent with known vision science on color vision deficiency. 3. Control experiment with a trichromat retina, but with cortical learning deliberately removed: *CMF-SIM* measures color as 1-D, highlighting that cortical learning is necessary for emergence of correct color dimensionality.

studies (Brettel et al., 1997) (yellow-blue hues for deuteranopia / protanopia (Judd, 1948; Graham & Hsia, 1959) and teal-pink hues for tritanopia (Alpern et al., 1983)) (Fig. 5.2).

In a control experiment, we verify that cortical learning is essential for color vision by comparing two scenarios: (1) a baseline where optic nerve signals directly form percepts, with all cortical learning deliberately removed (Fig. 5.3), and (2) the proposed model including cortical learning (Fig. 5.1, LMS case). The control baseline experiment fails standard color-matching tests, reducing color dimensionality to 1-D despite 3 cone types, demonstrating that cortical learning is indeed necessary for emergence of correct color dimensionality (details in Appendix D). In contrast, the proposed learning-based model results in correct 3-D color, as expected.

Figure 6 simulates boosting of color dimensionality in adulthood by gene therapy. Previous genetic studies (Jacobs et al., 2007; Mancuso et al., 2009; Zhang et al., 2017) demonstrated that the introduction of an additional class of photopigments in the mammalian cone mosaic, even in adulthood via gene therapy, resulted in a new dimension of chromatic sensory experience. Here, we simulate the experiment performed in squirrel monkeys (Mancuso et al., 2009), finding simulation results consistent with the noted boost in color dimensionality (Fig. 6.1). First, we model the vision of an adult male squirrel monkey with a protanopic retina (M and S cones only) and a cortical model that has converged. Next, we simulate the effects of gene therapy, by modifying the retina model so that a random subset of cones begin to express L opsin. Immediately after this retinal change, *NS* continues to show blue-yellow dichromatic vision. However, if we allow the cortical model to continue the hypothesized self-supervised learning, vision re-converges to boosted, 3-dimensional color (Fig. 6.1). As an aside, the real gene therapy experiment (Mancuso et al., 2009) resulted in expression of both M and L photopigment in affected cones, but the relative amounts are difficult to ascertain. We additionally model scenarios in which equal M and L expression occurs or a variable amount of L relative to M at each cell, and both scenarios converge to trichromacy as well (Appendix E). These result indicate that the hypothesized self-supervised learning can explain experimental boosting of color dimensionality in adulthood consistent with Mancuso et al. (2009), if the hypothesized learning is assumed to occur continuously even in adulthood.

Figure 6.B further demonstrates that simulations of boosting color dimensionality succeed even in 3D→4D cases by the addition of a fourth cone between S and M cones. This simulation results present the first theoretical work that highlights the possibility of boosting humans with trichromatic vision to tetrachromat one by addition of a fourth photopigment. Further details, including the study of human tetrachromat observer model, are described in Appendix F. We will release all the code and trained weights of our cortical model upon acceptance.

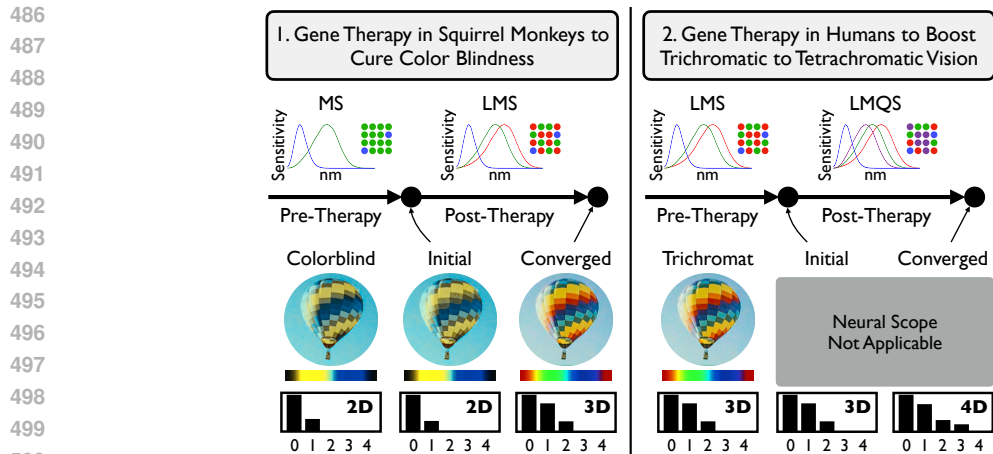


Figure 6: Simulated experiments for boosting color dimensionality via gene therapy. 1. A 2D dichromat color vision is boosted to 3D trichromacy by mutating some M cones to express L opsins, with cortical learning re-converging to 3D color. 2. Similarly, a 3D trichromat model is boosted to 4D tetrachromacy by adding a fourth cone type between M and L cones, with cortical learning re-converging to 4D color.

7 CONCLUSION

In this work, we presented a framework for modeling the emergence of color vision in the human brain. We introduced a simulation engine for optic nerve signals, simulated cortical learning purely from such input signals, and measured the emergent color dimensionality qualitatively with *NS* and quantitatively with *CMF-SIM*.

We believe that the critical contribution of this work actually lies in the computational formulation of the problem in human perception itself – given access to only a stream of optic nerve signals, we probe how to meaningfully model the emergence of color vision in the cortex via simulated learning. Once the problem is formulated this way, it may not be entirely surprising to machine learning researchers that color with the correct dimensionality can be inferred; however, from the vision science perspective, this new approach is in many ways a foreign way to formulate the problem, because it is more common to think color comes from hardwired neural circuits (Appendix D).

The connection to camera imaging systems is noteworthy as well. The proposed computational framework is akin to a camera processing pipeline attached to an unknown, random color filter array pattern, where even the number of different color filters is a mystery. This is related to a branch of computational imaging called “auto calibration” that jointly solves for the scene and unknown system calibration parameters from measurements. One could imagine a new class of engineered sensing systems that have general processing units along the lines of the learning mechanism in this paper, that enables perceptual inference from a broader range of sensory streams that do not require the precision manufacturing common to many current sensors and cameras.

The learning notion of perception emerging from a process of disentangling it from encoded sensory streams is an interesting intellectual view of how perception may generally emerge in the brain. Any sensory stream going to the brain encodes information from the world entangled with sensing organ characteristics. The self-supervised learning mechanism proposed in this paper might be abstracted into a general neural process of learning to predict fluctuations in sensory stream due to ego perturbation, with perception for that sense emerging neurally as the optimal internal representation and associated decoder/encoder pair that enables accurate prediction.

To conclude, we invite the research community to build on the computational framework proposed in this paper, by improving the visual system components (e.g. even more accurately modeling details in the eye model, or replacing back-propagation in the cortical model with more bio-plausible learning rules (Lillicrap et al., 2020; Hinton, 2022)), or applying the framework to other sensory modalities.

REFERENCES

- 540
541
542 *Colorimetry*. Number 15.2 in CIE Publication. Commission Internationale de l'Éclairage, Vienna,
543 Austria, 2nd edition, 1976.
- 544 Larry F Abbott. Lopicque's introduction of the integrate-and-fire model neuron (1907). *Brain*
545 *research bulletin*, 50(5-6):303–304, 1999.
- 546
547 Russell J Adams, Daphne Maurer, and Margaret Davis. Newborns' discrimination of chromatic from
548 achromatic stimuli. *Journal of Experimental Child Psychology*, 41(2):267–281, 1986.
- 549 Eirikur Agustsson and Radu Timofte. Ntire 2017 challenge on single image super-resolution:
550 Dataset and study. In *The IEEE Conference on Computer Vision and Pattern Recognition (CVPR)*
551 *Workshops*, July 2017.
- 552
553 Albert J Ahumada. Learning receptor positions. *Computational models of visual processing*, pp.
554 23–34, 1991.
- 555 M Alpern, K Kitahara, and D H Krantz. Perception of colour in unilateral tritanopia. *The Journal of*
556 *Physiology*, 335(1):683–697, 1983.
- 557
558 Alexander G Anderson, Kavitha Ratnam, Austin Roorda, and Bruno A Olshausen. High-acuity vision
559 from retinal image motion. *Journal of vision*, 20(7):34–34, 2020.
- 560 Juan M Angueyra, Jacob Baudin, Gregory W Schwartz, and Fred Rieke. Predicting and manipulating
561 cone responses to naturalistic inputs. *Journal of Neuroscience*, 42(7):1254–1274, 2022.
- 562
563 Boaz Arad, Radu Timofte, Rony Yahel, Nimrod Morag, Amir Bernat, Yuanhao Cai, Jing Lin, Zudi
564 Lin, Haoqian Wang, Yulun Zhang, et al. Ntire 2022 spectral recovery challenge and data set.
565 In *Proceedings of the IEEE/CVF Conference on Computer Vision and Pattern Recognition*, pp.
566 863–881, 2022.
- 567 Claudia Diaz Araya and Jan M Provis. Evidence of photoreceptor migration during early foveal
568 development: a quantitative analysis of human fetal retinae. *Visual neuroscience*, 8(6):505–514,
569 1992.
- 570
571 Michael A Arbib. *The handbook of brain theory and neural networks*. MIT press, 2003.
- 572 Manel Baradad, Jonas Wulff, Tongzhou Wang, Phillip Isola, and Antonio Torralba. Learning to see
573 by looking at noise. In *Advances in Neural Information Processing Systems*, 2021.
- 574
575 Horace B Barlow et al. Possible principles underlying the transformation of sensory messages.
576 *Sensory communication*, 1(01):217–233, 1961.
- 577 Bryce Bayer. Color imaging array. *United States Patent, no. 3971065*, 1976.
- 578
579 Noah C Benson, Jeremy R Manning, and David H Brainard. Unsupervised learning of cone spectral
580 classes from natural images. *PLoS Computational Biology*, 10(6):e1003652, 2014.
- 581
582 Michael J Berry, David K Warland, and Markus Meister. The structure and precision of retinal spike
583 trains. *Proceedings of the National Academy of Sciences*, 94(10):5411–5416, 1997.
- 584
585 Vicente Botella-Soler, Stéphane Deny, Georg Martius, Olivier Marre, and Gašper Tkačič. Nonlinear
586 decoding of a complex movie from the mammalian retina. *PLoS computational biology*, 14(5):
587 e1006057, 2018.
- 588
589 Nora Brackbill, Colleen Rhoades, Alexandra Kling, Nishal P Shah, Alexander Sher, Alan M Litke,
590 and EJ Chichilnisky. Reconstruction of natural images from responses of primate retinal ganglion
591 cells. *Elife*, 9:e58516, 2020.
- 592
593 David Brainard, Haomiao Jiang, Nicolas P Cottaris, Fred Rieke, EJ Chichilnisky, Joyce E Farrell,
and Brian A Wandell. Isetbio: Computational tools for modeling early human vision. In *Imaging*
Systems and Applications, pp. IT4A–4. Optica Publishing Group, 2015.
- David H Brainard. Color and the cone mosaic. *Annual Review of Vision Science*, 1:519–546, 2015.

- 594 David H Brainard, David R Williams, and Heidi Hofer. Trichromatic reconstruction from the
595 interleaved cone mosaic: Bayesian model and the color appearance of small spots. *Journal of*
596 *vision*, 8(5):15–15, 2008.
- 597
598 Hans Brettel, Françoise Viénot, and John D Mollon. Computerized simulation of color appearance
599 for dichromats. *Josa a*, 14(10):2647–2655, 1997.
- 600
601 Gijs Joost Brouwer and David J Heeger. Decoding and reconstructing color from responses in human
602 visual cortex. *Journal of Neuroscience*, 29(44):13992–14003, 2009.
- 603
604 Angela M Brown. Development of visual sensitivity to light and color vision in human infants: A
605 critical review. *Vision Research*, 30(8):1159–1188, 1990.
- 606
607 Yoram Burak, Uri Rokni, Markus Meister, and Haim Sompolinsky. Bayesian model of dynamic
608 image stabilization in the visual system. *Proceedings of the National Academy of Sciences*, 107
(45):19525–19530, 2010.
- 609
610 Joseph Carroll, Carrie McMahon, Maureen Neitz, and Jay Neitz. Flicker-photometric electroretino-
611 gram estimates of l: M cone photoreceptor ratio in men with photopigment spectra derived from
612 genetics. *JOSA A*, 17(3):499–509, 2000.
- 613
614 Joseph Carroll, Jay Neitz, and Maureen Neitz. Estimates of l: M cone ratio from erg flicker photometry
and genetics. *Journal of vision*, 2(8):1–1, 2002.
- 615
616 Ting Chen, Simon Kornblith, Mohammad Norouzi, and Geoffrey Hinton. A simple framework for
617 contrastive learning of visual representations. In *International conference on machine learning*, pp.
618 1597–1607. PMLR, 2020.
- 619
620 CIE. Commission internationale de l’éclairage proceedings, 1931.
- 621
622 Bevil R Conway. The organization and operation of inferior temporal cortex. *Annual review of vision*
science, 4:381–402, 2018.
- 623
624 Bevil R Conway, Saima Malik-Moraleda, and Edward Gibson. Color appearance and the end of
625 hering’s opponent-colors theory. *Trends in Cognitive Sciences*, 2023.
- 626
627 Frans W Cornelissen and Eli Brenner. Is adding a new class of cones to the retina sufficient to cure
color-blindness? *Journal of vision*, 15(13):22–22, 2015.
- 628
629 Nicolas P Cottaris, Haomiao Jiang, Xiaomao Ding, Brian A Wandell, and David H Brainard. A
630 computational-observer model of spatial contrast sensitivity: Effects of wave-front-based optics,
631 cone-mosaic structure, and inference engine. *Journal of vision*, 19(4):8–8, 2019.
- 632
633 Lisa J Croner and Ehud Kaplan. Receptive fields of p and m ganglion cells across the primate retina.
Vision research, 35(1):7–24, 1995.
- 634
635 Joanna D Crook, Orin S Packer, John B Troy, and Dennis M Dacey. Synaptic mechanisms of color
636 and luminance coding: rediscovering the xy-cell dichotomy in primate retinal ganglion cells. In
637 *The new visual neurosciences*, pp. 123–144. The MIT Press, Cambridge, MA, 2013.
- 638
639 Christine A Curcio, Kenneth R Sloan, Robert E Kalina, and Anita E Hendrickson. Human photore-
ceptor topography. *Journal of comparative neurology*, 292(4):497–523, 1990.
- 640
641 Dennis Dacey, Orin S Packer, Lisa Diller, David Brainard, Beth Peterson, and Barry Lee. Center
642 surround receptive field structure of cone bipolar cells in primate retina. *Vision research*, 40(14):
643 1801–1811, 2000.
- 644
645 Dennis M Dacey. The mosaic of midget ganglion cells in the human retina. *Journal of Neuroscience*,
13(12):5334–5355, 1993.
- 646
647 Dennis M Dacey and Barry B Lee. The ‘blue-on’ opponent pathway in primate retina originates from
a distinct bistratified ganglion cell type. *Nature*, 367(6465):731–735, 1994.

- 648 Dennis M Dacey, Barry B Lee, Donna K Stafford, Joel Pokorny, and Vivianne C Smith. Horizontal
649 cells of the primate retina: cone specificity without spectral opponency. *Science*, 271(5249):
650 656–659, 1996.
- 651 Virginia De Sa. Learning classification with unlabeled data. *Advances in neural information
652 processing systems*, 6, 1993.
- 654 Russell L De Valois and Karen K De Valois. A multi-stage color model. *Vision research*, 33(8):
655 1053–1065, 1993.
- 656 Andrew M Derrington, John Krauskopf, and Peter Lennie. Chromatic mechanisms in lateral geniculate
657 nucleus of macaque. *The Journal of physiology*, 357(1):241–265, 1984.
- 659 René Descartes. *Descartes: Selected philosophical writings*. Cambridge University Press, 1988.
- 660 Laurent Dinh, Jascha Sohl-Dickstein, and Samy Bengio. Density estimation using real nvp. *arXiv
661 preprint arXiv:1605.08803*, 2016.
- 663 Robert F Dougherty, Volker M Koch, Alyssa A Brewer, Bernd Fischer, Jan Modersitzki, and Brian A
664 Wandell. Visual field representations and locations of visual areas v1/2/3 in human visual cortex.
665 *Journal of vision*, 3(10):1–1, 2003.
- 666 John E Dowling and Brian Blundell Boycott. Organization of the primate retina: electron microscopy.
667 *Proceedings of the Royal Society of London. Series B. Biological Sciences*, 166(1002):80–111,
668 1966.
- 670 Ch Enroth-Cugell, JG Robson, DE Schweitzer-Tong, and AB Watson. Spatio-temporal interactions
671 in cat retinal ganglion cells showing linear spatial summation. *The Journal of Physiology*, 341(1):
672 279–307, 1983.
- 673 Mark D Fairchild. *Color appearance models*. John Wiley & Sons, 2013.
- 674 Greg D Field, Jeffrey L Gauthier, Alexander Sher, Martin Greschner, Timothy A Machado, Lauren H
675 Jepson, Jonathon Shlens, Deborah E Gunning, Keith Mathieson, Wladyslaw Dabrowski, et al.
676 Functional connectivity in the retina at the resolution of photoreceptors. *Nature*, 467(7316):
677 673–677, 2010.
- 679 Peter Földiák. Learning invariance from transformation sequences. *Neural computation*, 3(2):
680 194–200, 1991.
- 682 Eric R Fossum. Cmos image sensors: Electronic camera-on-a-chip. *IEEE transactions on electron
683 devices*, 44(10):1689–1698, 1997.
- 684 David H. Foster. Color constancy. *Vision Research*, 51(7):674–700, 2011. ISSN 0042-6989. doi:
685 <https://doi.org/10.1016/j.visres.2010.09.006>. Vision Research 50th Anniversary Issue: Part 1.
- 687 Julian Freedland and Fred Rieke. Systematic reduction of the dimensionality of natural scenes allows
688 accurate predictions of retinal ganglion cell spike outputs. *Proceedings of the National Academy
689 of Sciences*, 119(46):e2121744119, 2022.
- 690 Tyler Godat, Nicolas P Cottaris, Sara Patterson, Kendall Kohout, Keith Parkins, Qiang Yang, Jen-
691 nifer M Strazzeri, Juliette E McGregor, David H Brainard, William H Merigan, et al. In vivo
692 chromatic and spatial tuning of foveolar retinal ganglion cells in macaca fascicularis. *Plos one*, 17
693 (11):e0278261, 2022.
- 694 CH Graham and Yun Hsia. Studies of color blindness: a unilaterally dichromatic subject, 1959.
- 696 Hermann Grassmann. Zur theorie der farbenmischung. *Annalen der Physik*, 165(5):69–84, 1853.
- 697 John Guild. The colorimetric properties of the spectrum. *Philosophical Transactions of the Royal
698 Society of London. Series A, Containing Papers of a Mathematical or Physical Character*, 230
699 (681-693):149–187, 1931.
- 700 S Lee Guth. Model for color vision and light adaptation. *JOSA A*, 8(6):976–993, 1991.
- 701

- 702 Theodros M Haile, Kaitlin S Bohon, Maria C Romero, and Bevil R Conway. Visual stimulus-driven
703 functional organization of macaque prefrontal cortex. *Neuroimage*, 188:427–444, 2019.
704
- 705 H KEFFER Hartline and Floyd Ratliff. Spatial summation of inhibitory influences in the eye of
706 limulus, and the mutual interaction of receptor units. *The Journal of general physiology*, 41(5):
707 1049–1066, 1958.
- 708 Kaiming He, Xinlei Chen, Saining Xie, Yanghao Li, Piotr Dollár, and Ross Girshick. Masked
709 autoencoders are scalable vision learners. In *Proceedings of the IEEE/CVF conference on computer
710 vision and pattern recognition*, pp. 16000–16009, 2022.
711
- 712 Ewald Hering. *Zur Lehre vom Lichtsinne: sechs Mittheilungen an die Kaiserl. Akademie der
713 Wissenschaften in Wien*. C. Gerold’s Sohn, 1878.
- 714 Geoffrey Hinton. The forward-forward algorithm: Some preliminary investigations. *arXiv preprint
715 arXiv:2212.13345*, 2022.
716
- 717 Geoffrey E Hinton. Connectionist learning procedures. In *Machine learning*, pp. 555–610. Elsevier,
718 1990.
- 719 Hajime Hirasawa and Akimichi Kaneko. pH Changes in the Invaginating Synaptic Cleft Mediate
720 Feedback from Horizontal Cells to Cone Photoreceptors by Modulating Ca²⁺ Channels. *Journal
721 of General Physiology*, 122(6):657–671, 11 2003. ISSN 0022-1295.
- 722 Heidi Hofer, Joseph Carroll, Jay Neitz, Maureen Neitz, and David R Williams. Organization of the
723 human trichromatic cone mosaic. *Journal of Neuroscience*, 25(42):9669–9679, 2005.
724
- 725 Gordon Holmes. Disturbances of vision by cerebral lesions. *The British journal of ophthalmology*, 2
726 (7):353, 1918.
- 727 David H Hubel and Torsten N Wiesel. Receptive fields, binocular interaction and functional architec-
728 ture in the cat’s visual cortex. *The Journal of physiology*, 160(1):106, 1962.
729
- 730 Gerald H Jacobs. Photopigments and the dimensionality of animal color vision. *Neuroscience &
731 Biobehavioral Reviews*, 86:108–130, 2018.
- 732 Gerald H Jacobs, Gary A Williams, Hugh Cahill, and Jeremy Nathans. Emergence of novel color
733 vision in mice engineered to express a human cone photopigment. *science*, 315(5819):1723–1725,
734 2007.
735
- 736 Sandra Jiménez and Jesús Malo. The role of spatial information in disentangling the irradiance–
737 reflectance–transmittance ambiguity. *IEEE transactions on geoscience and remote sensing*, 52(8):
738 4881–4894, 2013.
- 739 Gabriele Jordan, Samir S Deeb, Jenny M Bosten, and John D Mollon. The dimensionality of color
740 vision in carriers of anomalous trichromacy. *Journal of vision*, 10(8):12–12, 2010.
741
- 742 Deane B Judd. Color perceptions of deuteranopic and protanopic observers. *Journal of Research of
743 the National Bureau of Standards*, 41:247–271, 1948.
- 744 Deane B Judd. *Response functions for types of vision according to the Müller theory*. US Government
745 Printing Office, 1949.
746
- 747 Young Joon Kim, Nora Brackbill, Eleanor Batty, JinHyung Lee, Catalin Mitelut, William Tong,
748 EJ Chichilnisky, and Liam Paninski. Nonlinear decoding of natural images from large-scale
749 primate retinal ganglion recordings. *Neural Computation*, 33(7):1719–1750, 2021.
- 750 Ron Kimmel. Demosaicing: Image reconstruction from color ccd samples. *IEEE Transactions on
751 image processing*, 8(9):1221–1228, 1999.
- 752 Diederik P Kingma and Jimmy Ba. Adam: A method for stochastic optimization. *arXiv preprint
753 arXiv:1412.6980*, 2014.
754
- 755 John Krauskopf and Gegenfurtner Karl. Color discrimination and adaptation. *Vision research*, 32
(11):2165–2175, 1992.

- 756 Stephen W Kuffler. Discharge patterns and functional organization of mammalian retina. *Journal of*
757 *neurophysiology*, 16(1):37–68, 1953.
758
- 759 Rosa Lafer-Sousa and Bevil R Conway. Parallel, multi-stage processing of colors, faces and shapes
760 in macaque inferior temporal cortex. *Nature neuroscience*, 16(12):1870–1878, 2013.
761
- 762 Edwin H Land. The retinex theory of color vision. *Scientific american*, 237(6):108–129, 1977.
763
- 764 Michael F Land and Dan-Eric Nilsson. *Animal eyes*. OUP Oxford, 2012.
765
- 766 L Lapicque. Recherches quantitatives sur l’excitation électrique des nerfs. *J. Physiol. Paris*, 9:
620–635, 1907.
767
- 768 Jessica Lee, Nicholas Jennings, Varun Srivastava, and Ren Ng. Theory of human tetrachromatic color
769 experience and printing. *ACM Trans. Graph*, 43(4), July 2024.
770
- 771 Peter Lennie, P William Haake, and David R Williams. The design of chromatically opponent
772 receptive fields. *Computational models of visual processing*, pp. 71–82, 1991.
773
- 774 Ming Li, Fang Liu, Mikko Juusola, and Shiming Tang. Perceptual color map in macaque visual area
v4. *Journal of Neuroscience*, 34(1):202–217, 2014.
775
- 776 Trisha Lian, Kevin J MacKenzie, David H Brainard, Nicolas P Cottaris, and Brian A Wandell. Ray
777 tracing 3d spectral scenes through human optics models. *Journal of vision*, 19(12):23–23, 2019.
778
- 779 Timothy P Lillicrap, Adam Santoro, Luke Marris, Colin J Akerman, and Geoffrey Hinton. Backprop-
780 agation and the brain. *Nature Reviews Neuroscience*, 21(6):335–346, 2020.
781
- 782 AM Litke, N Bezayiff, EJ Chichilnisky, W Cunningham, W Dabrowski, AA Grillo, M Grivich,
783 P Grybos, P Hottowy, S Kachiguine, et al. What does the eye tell the brain?: Development of
784 a system for the large-scale recording of retinal output activity. *IEEE Transactions on Nuclear*
Science, 51(4):1434–1440, 2004.
785
- 786 Jian K Liu, Dimokratis Karamanlis, and Tim Gollisch. Simple model for encoding natural images
787 by retinal ganglion cells with nonlinear spatial integration. *PLoS computational biology*, 18(3):
e1009925, 2022.
788
- 789 Jianfei Liu, HaeWon Jung, Alfredo Dubra, and Johnny Tam. Cone photoreceptor cell segmentation
790 and diameter measurement on adaptive optics images using circularly constrained active contour
791 model. *Investigative ophthalmology & visual science*, 59(11):4639–4652, 2018.
792
- 793 Ye Liu, Ming Li, Xian Zhang, Yiliang Lu, Hongliang Gong, Jiapeng Yin, Zheyuan Chen, Liling
794 Qian, Yupeng Yang, Ian Max Andolina, et al. Hierarchical representation for chromatic processing
795 across macaque v1, v2, and v4. *Neuron*, 108(3):538–550, 2020.
796
- 797 Margaret S Livingstone and David H Hubel. Psychophysical evidence for separate channels for the
798 perception of form, color, movement, and depth. *Journal of Neuroscience*, 7(11):3416–3468, 1987.
799
- 800 William Lotter, Gabriel Kreiman, and David Cox. Deep predictive coding networks for video
801 prediction and unsupervised learning. In *International Conference on Learning Representations*,
2016.
802
- 803 David L MacAdam. Visual sensitivities to color differences in daylight. *Josa*, 32(5):247–274, 1942.
804
- 805 Donald IA MacLeod and Robert M Boynton. Chromaticity diagram showing cone excitation by
806 stimuli of equal luminance. *JOSA*, 69(8):1183–1186, 1979.
807
- 808 Walter Makous. Comment on " emergence of novel color vision in mice engineered to express a
809 human cone photopigment". *Science*, 318(5848):196–196, 2007.
- 809 Laurence T Maloney and Albert J Ahumada. Learning by assertion: Two methods for calibrating a
linear visual system. *Neural Computation*, 1(3):392–401, 1989.

- 810 Katherine Mancuso, William W Hauswirth, Qihong Li, Thomas B Connor, James A Kuchenbecker,
811 Matthew C Mauck, Jay Neitz, and Maureen Neitz. Gene therapy for red–green colour blindness in
812 adult primates. *Nature*, 461(7265):784–787, 2009.
- 813 Olivier Marre, Gasper Tkacik, Dario Amodei, Elad Schneidman, William Bialek, and Michael Berry.
814 Multi-electrode array recording from salamander retinal ganglion cells. 2017.
- 815
816 Susana Martinez-Conde, Jorge Otero-Millan, and Stephen L Macknik. The impact of microsaccades
817 on vision: towards a unified theory of saccadic function. *Nature Reviews Neuroscience*, 14(2):
818 83–96, 2013.
- 819 James Clerk Maxwell. Theory of the perception of colors. *Trans. R. Scottish Soc. Arts*, 4:394–400,
820 1856.
- 821
822 J. W. McClurkin and L. M. Optican. Primate striate and prestriate cortical neurons during discrim-
823 ination. i. simultaneous temporal encoding of information about color and pattern. *Journal of*
824 *Neurophysiology*, 75(1):481–495, 1996.
- 825 J. W. McClurkin, J. A. Zarbock, and L. M Optican. Primate striate and prestriate cortical neurons dur-
826 ing discrimination. ii. separable temporal codes for color and pattern. *Journal of Neurophysiology*,
827 75(1):496–507, 1996.
- 828
829 K McLaren. Xiii—the development of the cie 1976 (1* a* b*) uniform colour space and colour-
830 difference formula. *Journal of the Society of Dyers and Colourists*, 92(9):338–341, 1976.
- 831 Matthew J McMahon, Martin JM Lankheet, Peter Lennie, and David R Williams. Fine structure of
832 parvocellular receptive fields in the primate fovea revealed by laser interferometry. *Journal of*
833 *Neuroscience*, 20(5):2043–2053, 2000.
- 834
835 JD Mollon and JK Bowmaker. The spatial arrangement of cones in the primate fovea. *Nature*, 360
836 (6405):677–679, 1992.
- 837 Thomas Naselaris, Ryan J Prenger, Kendrick N Kay, Michael Oliver, and Jack L Gallant. Bayesian
838 reconstruction of natural images from human brain activity. *Neuron*, 63(6):902–915, 2009.
- 839
840 J Neitz and M Neitz. Evolution of the circuitry for conscious color vision in primates. *Eye*, 31(2):
841 286–300, 2017.
- 842 Jay Neitz and Maureen Neitz. The genetics of normal and defective color vision. *Vision Research*, 51
843 (7):633–651, 2011.
- 844
845 Isaac Newton. *Opticks: or, A Treatise of the Reflexions, Refractions, Inflexions and Colours of Light*.
846 Courier Corporation, 1704.
- 847 Shinji Nishimoto, An T Vu, Thomas Naselaris, Yuval Benjamini, Bin Yu, and Jack L Gallant.
848 Reconstructing visual experiences from brain activity evoked by natural movies. *Current biology*,
849 21(19):1641–1646, 2011.
- 850
851 J Kevin O’Regan and Alva Noë. A sensorimotor account of vision and visual consciousness.
852 *Behavioral and brain sciences*, 24(5):939–973, 2001.
- 853
854 Gustav A Osterberg. Topography of the layer of rods and cones in the human retina. *Acta ophthalmo-*
855 *logica*, 1935.
- 856
857 Orin S Packer and Dennis M Dacey. Receptive field structure of h1 horizontal cells in macaque
858 monkey retina. *Journal of Vision*, 2(4):1–1, 2002.
- 859
860 Stephanie E Palmer, Olivier Marre, Michael J Berry, and William Bialek. Predictive information in a
861 sensory population. *Proceedings of the National Academy of Sciences*, 112(22):6908–6913, 2015.
- 862
863 Nikhil Parthasarathy, Eleanor Batty, William Falcon, Thomas Rutten, Mohit Rajpal, EJ Chichilnisky,
and Liam Paninski. Neural networks for efficient bayesian decoding of natural images from retinal
neurons. *Advances in Neural Information Processing Systems*, 30, 2017.
- Ken Perlin. An image synthesizer. *ACM Siggraph Computer Graphics*, 19(3):287–296, 1985.

- 864 Baingio Pinna. Un effetto di colorazione. In *Il laboratorio e la città. XXI Congresso degli Psicologi*
865 *Italiani*, volume 158. Edizioni SIPs, Società Italiana di Psicologia, Milano, 1987.
866
- 867 Baingio Pinna, Gavin Brelstaff, and Lothar Spillmann. Surface color from boundaries: a new
868 ‘watercolor’ illusion. *Vision research*, 41(20):2669–2676, 2001.
- 869 Jonathan R Polimeni, Bruce Fischl, Douglas N Greve, and Lawrence L Wald. Laminar analysis of 7
870 t bold using an imposed spatial activation pattern in human v1. *Neuroimage*, 52(4):1334–1346,
871 2010.
- 872 Rajeev Ramanath, Wesley E Snyder, Griff L Bilbro, and William A Sander III. Demosaicking
873 methods for bayer color arrays. *Journal of Electronic imaging*, 11(3):306–315, 2002.
874
- 875 Rajesh PN Rao and Dana H Ballard. Predictive coding in the visual cortex: a functional interpretation
876 of some extra-classical receptive-field effects. *Nature neuroscience*, 2(1):79–87, 1999.
877
- 878 Katja Reinhard and Thomas A Münch. Visual properties of human retinal ganglion cells. *PLoS One*,
879 16(2):e0246952, 2021.
- 880 Ilias Rentzeperis, Andrey R Nikolaev, Daniel C Kiper, and Cees van Leeuwen. Distributed processing
881 of color and form in the visual cortex. *Frontiers in psychology*, 5:932, 2014.
882
- 883 Dragos L Rezeanu, James Kuchenbecker, Rachel Barborek, Marcus Mazzaferri, Maureen Neitz, and
884 Jay Neitz. Explaining the absence of functional tetrachromacy in females with four cone types.
885 *Investigative Ophthalmology & Visual Science*, 62(8):527–527, 2021.
- 886 Danilo Rezende and Shakir Mohamed. Variational inference with normalizing flows. In *International*
887 *conference on machine learning*, pp. 1530–1538. PMLR, 2015.
888
- 889 Austin H Riesen, Robert L Ramsey, and Paul D Wilson. Development of visual acuity in rhesus
890 monkeys deprived of patterned light during early infancy. *Psychonomic Science*, 1(1-12):33–34,
891 1964.
- 892 Mattia Rigotti, Omri Barak, Melissa R Warden, Xiao-Jing Wang, Nathaniel D Daw, Earl K Miller,
893 and Stefano Fusi. The importance of mixed selectivity in complex cognitive tasks. *Nature*, 497
894 (7451):585–590, 2013.
- 895 Robert W Rodieck. Quantitative analysis of cat retinal ganglion cell response to visual stimuli. *Vision*
896 *research*, 5(12):583–601, 1965.
897
- 898 Robert W Rodieck. The first steps in seeing. 1998.
- 899 Martin Rolfs. Microsaccades: small steps on a long way. *Vision research*, 49(20):2415–2441, 2009.
900
- 901 Olaf Ronneberger, Philipp Fischer, and Thomas Brox. U-net: Convolutional networks for biomedical
902 image segmentation. In *Medical Image Computing and Computer-Assisted Intervention–MICCAI*
903 *2015: 18th International Conference, Munich, Germany, October 5-9, 2015, Proceedings, Part III*
904 *18*, pp. 234–241. Springer, 2015.
- 905 Austin Roorda, Fernando Romero-Borja, William J Donnelly III, Hope Queener, Thomas J Hebert,
906 and Melanie CW Campbell. Adaptive optics scanning laser ophthalmoscopy. *Optics express*, 10
907 (9):405–412, 2002.
- 908 Michele Rucci and Jonathan D Victor. The unsteady eye: an information-processing stage, not a bug.
909 *Trends in neurosciences*, 38(4):195–206, 2015.
910
- 911 Michele Rucci, Ehud Ahissar, and David Burr. Temporal coding of visual space. *Trends in cognitive*
912 *sciences*, 22(10):883–895, 2018.
- 913 Ramkumar Sabesan, Heidi Hofer, and Austin Roorda. Characterizing the human cone photoreceptor
914 mosaic via dynamic photopigment densitometry. *PLoS one*, 10(12):e0144891, 2015.
915
- 916 Ramkumar Sabesan, Brian P Schmidt, William S Tuten, and Austin Roorda. The elementary
917 representation of spatial and color vision in the human retina. *Science advances*, 2(9):e1600797,
2016.

- 918 Jared M Salisbury and Stephanie E Palmer. Optimal prediction in the retina and natural motion
919 statistics. *Journal of Statistical Physics*, 162(5):1309–1323, 2016.
920
- 921 Elad Schneidman, Michael J Berry, Ronen Segev, and William Bialek. Weak pairwise correlations
922 imply strongly correlated network states in a neural population. *Nature*, 440(7087):1007–1012,
923 2006.
- 924 Manuel Schottdorf and Barry B Lee. A quantitative description of macaque ganglion cell responses
925 to natural scenes: the interplay of time and space. *The Journal of physiology*, 599(12):3169–3193,
926 2021.
927
- 928 Jérémie Sibille, Carolin Gehr, Jonathan I Benichov, Hymavathy Balasubramanian, Kai Lun Teh,
929 Tatiana Lupashina, Daniela Vallentin, and Jens Kremkow. High-density electrode recordings reveal
930 strong and specific connections between retinal ganglion cells and midbrain neurons. *Nature*
931 *communications*, 13(1):5218, 2022.
- 932 Yosef Singer, Yayoi Teramoto, Ben DB Willmore, Jan WH Schnupp, Andrew J King, and Nicol S
933 Harper. Sensory cortex is optimized for prediction of future input. *elife*, 7:e31557, 2018.
934
- 935 Yosef Singer, Luke Taylor, Ben DB Willmore, Andrew J King, and Nicol S Harper. Hierarchical
936 temporal prediction captures motion processing along the visual pathway. *eLife*, 12:e52599, 2023a.
937
- 938 Yosef Singer, Luke Taylor, Ben DB Willmore, Andrew J King, and Nicol S Harper. Hierarchical
939 temporal prediction captures motion processing along the visual pathway. *Elife*, 12:e52599, 2023b.
- 940 Barun Singh, William T Freeman, and D Brainard. Exploiting spatial and spectral image regularities
941 for color constancy. In *Workshop on Statistical and Computational Theories of Vision. Nice, France*.
942 Citeseer, 2003.
- 943
- 944 Florentina Soto, Jen-Chun Hsiang, Rithwick Rajagopal, Kisha Piggott, George J Harocopos, Steven M
945 Couch, Philip Custer, Josh L Morgan, and Daniel Kerschensteiner. Efficient coding by midget and
946 parasol ganglion cells in the human retina. *Neuron*, 107(4):656–666, 2020.
- 947 Mandyam Veerambudi Srinivasan, Simon Barry Laughlin, and Andreas Dubs. Predictive coding:
948 a fresh view of inhibition in the retina. *Proceedings of the Royal Society of London. Series B*.
949 *Biological Sciences*, 216(1205):427–459, 1982.
950
- 951 WS Stiles and JM Burch. Interim report to the commission internationale de l’éclairage, zurich,
952 1955, on the national physical laboratory’s investigation of colour-matching (1955). *Optica Acta*:
953 *International Journal of Optics*, 2(4):168–181, 1955.
- 954 Vincent Stimper, David Liu, Andrew Campbell, Vincent Berenz, Lukas Ryll, Bernhard Schölkopf,
955 and José Miguel Hernández-Lobato. normflows: A pytorch package for normalizing flows.
956 *Journal of Open Source Software*, 8(86):5361, 2023. doi: 10.21105/joss.05361. URL <https://doi.org/10.21105/joss.05361>.
957
- 958 Andrew Stockman and Lindsay T Sharpe. The spectral sensitivities of the middle-and long-
959 wavelength-sensitive cones derived from measurements in observers of known genotype. *Vision*
960 *research*, 40(13):1711–1737, 2000.
961
- 962 Andrew Stockman, Lindsay T. Sharpe, and Clemens Fach. The spectral sensitivity of the human
963 short-wavelength sensitive cones derived from thresholds and color matches. *Vision Research*, 39
964 (17):2901–2927, 1999. ISSN 0042-6989.
- 965 Andrew Stockman, David H Brainard, et al. Color vision mechanisms. *OSA handbook of optics*, 3:
966 11–1, 2010.
967
- 968 Roger BH Tootell, Martin S Silverman, Eugene Switkes, and Russell L De Valois. Deoxyglucose
969 analysis of retinotopic organization in primate striate cortex. *Science*, 218(4575):902–904, 1982.
970
- 971 Antonio Torralba and Aude Oliva. Statistics of natural image categories. *Network: computation in*
neural systems, 14(3):391, 2003.

- 972 Ashish Vaswani, Noam Shazeer, Niki Parmar, Jakob Uszkoreit, Llion Jones, Aidan N Gomez, Łukasz
973 Kaiser, and Illia Polosukhin. Attention is all you need. *Advances in neural information processing*
974 *systems*, 30, 2017.
- 975
976 Jan Verweij, Eric P Hornstein, and Julie L Schnapf. Surround antagonism in macaque cone photore-
977 ceptors. *Journal of Neuroscience*, 23(32):10249–10257, 2003.
- 978
979 Hermann Von Helmholtz. *Handbuch der physiologischen Optik*, volume 9. Voss, 1867.
- 980
981 J Von Kries. Theoretische studien über die umstimmung des sehorgans. *Festschrift der Albrecht-*
982 *Ludwigs-Universität*, 32:145–158, 1902.
- 983
984 Thomas Wachtler, Eizaburo Doi, Te-Won Lee, and Terrence J Sejnowski. Cone selectivity derived
985 from the responses of the retinal cone mosaic to natural scenes. *Journal of vision*, 7(8):6–6, 2007.
- 986
987 GEORGE WALD. The molecular basis of visual excitation. *Nature*, 219(5156):800–807, 1968.
- 988
989 Yiyi Wang, Nicolas Bensaïd, Pavan Tiruveedhula, Jianqiang Ma, Sowmya Ravikumar, and Austin
990 Roorda. Human foveal cone photoreceptor topography and its dependence on eye length. *Elife*, 8:
991 e47148, 2019.
- 992
993 John S Werner, Brennan Marsh-Armstrong, and Kenneth Knoblauch. Adaptive changes in color
994 vision from long-term filter usage in anomalous but not normal trichromacy. *Current Biology*, 30
995 (15):3011–3015, 2020.
- 996
997 David R Williams, Donald IA MacLeod, and Mary M Hayhoe. Foveal tritanopia. *Vision Research*,
998 21(9):1341–1356, 1981.
- 999
1000 Lance Williams. Pyramidal parametrics. In *Proceedings of the 10th annual conference on Computer*
1001 *graphics and interactive techniques*, pp. 1–11, 1983.
- 1002
1003 Lauren E Wool, Joanna D Crook, John B Troy, Orin S Packer, Qasim Zaidi, and Dennis M Dacey.
1004 Nonselective wiring accounts for red-green opponency in midget ganglion cells of the primate
1005 retina. *Journal of Neuroscience*, 38(6):1520–1540, 2018.
- 1006
1007 William David Wright. A re-determination of the trichromatic coefficients of the spectral colours.
1008 *Transactions of the Optical Society*, 30(4):141, 1929.
- 1009
1010 Eric Wu, Nora Brackbill, Alexander Sher, Alan Litke, Eero Simoncelli, and EJ Chichilnisky. Maxi-
1011 mum a posteriori natural scene reconstruction from retinal ganglion cells with deep denoiser priors.
1012 *Advances in Neural Information Processing Systems*, 35:27212–27224, 2022.
- 1013
1014 Günther Wyszecki and Walter Stanley Stiles. *Color science: concepts and methods, quantitative data*
1015 *and formulae*. John wiley & sons, 1982.
- 1016
1017 Ed Yong. *An immense world: How animal senses reveal the hidden realms around us*. Knopf Canada,
1018 2022.
- 1019
1020 Laura K Young and Hannah E Smithson. Emulated retinal image capture (erica) to test, train and
1021 validate processing of retinal images. *Scientific Reports*, 11(1):11225, 2021.
- 1022
1023 Thomas Young. Ii. the bakerian lecture. on the mechanism of the eye. *Philosophical Transactions of*
1024 *the Royal Society of London*, (91):23–88, 1801.
- 1025
1026 Thomas Young. Ii. the bakerian lecture. on the theory of light and colours. *Philosophical transactions*
1027 *of the Royal Society of London*, (92):12–48, 1802.
- 1028
1029 Semir M Zeki. Functional specialisation in the visual cortex of the rhesus monkey. *Nature*, 274
1030 (5670):423–428, 1978.
- 1031
1032 Ling-Qi Zhang, Nicolas P Cottaris, and David H Brainard. An image reconstruction framework for
1033 characterizing initial visual encoding. *Elife*, 11:e71132, 2022.

1026 Yuxin Zhang, Wen-Tao Deng, Wei Du, Ping Zhu, Jie Li, Fan Xu, Jingfen Sun, Cecilia D Gerstner,
1027 Wolfgang Baehr, Sanford L Boye, et al. Gene-based therapy in a mouse model of blue cone
1028 monochromacy. *Scientific reports*, 7(1):6690, 2017.
1029
1030 Zhetuo Zhao, Ehud Ahissar, Jonathan D Victor, and Michele Rucci. Inferring visual space from
1031 ultra-fine extra-retinal knowledge of gaze position. *Nature communications*, 14(1):269, 2023.
1032
1033
1034
1035
1036
1037
1038
1039
1040
1041
1042
1043
1044
1045
1046
1047
1048
1049
1050
1051
1052
1053
1054
1055
1056
1057
1058
1059
1060
1061
1062
1063
1064
1065
1066
1067
1068
1069
1070
1071
1072
1073
1074
1075
1076
1077
1078
1079